Histol Histopathol (2019) 34: 57-67

http://www.hh.um.es

Histology and Histopathology

From Cell Biology to Tissue Engineering

Type 1 diabetes mellitus induced low bone turnover in ovariectomized rats

Bo Liu[1,2]* Wei Feng[2,3]*, Tomoka Hasegawa[4], Norio Amizuka[4] and Minqi Li[2]

[1]Department of Stomatology, Jining Medical University, [2]Department of Bone Metabolism, School of Stomatology Shandong University, Shandong Provincial Key Laboratory of Oral Tissue Regeneration, [3]Department of Endodontics, Jinan Stomatological Hospital, Jinan, China and [4]Department of Developmental Biology of Hard Tissue, Graduate School of Dental Medicine, Hokkaido University, Sapporo, Japan

*Bo Liu and Wei Feng have equaly contributed to this article

Summary. To investigate type 1 diabetes mellitus (T1DM) affecting bone remodeling in the context of menopause in female rats. The animals were subjected to either ovariectomy (OVX) which was performed to mimic postmenopausal estrogen deficiency, and/or type 1 diabetes mellitus which was established by the intra-abdominal administration of 50 mg/kg streptozotocin (STZ). Single-loaded groups were the OVX group and the STZ group, while the combined group was the OVX+STZ group. Bone histomorphometry was performed on the tibial metaphysis by Micro-CT scanning. Immunohistochemistry was used to assess the activity of osteoblast and osteoclast by counteracting with antibodies against their respective specific marker enzymes. The gene expression of key molecules involved in osteoblastic and osteoclastic signaling pathways were analyzed by RT-qPCR. The results showed a significant bone volume decrease in both single-loaded groups and combined group with the combined group suffering greatest bone loss and bone structural deterioration ($p<0.001$). Immunohistochemical staining and RT-qPCR revealed an increase in osteoblastic ($p<0.001$) and osteoclastic ($p<0.01$) activities in OVX rats while there was a decrease ($p<0.05$) in those of STZ rats. When OVX and STZ were combined, the rats exhibited a further decrease in osteoblastic activity ($p<0.001$) and a similar level of osteoclastic activity ($p>0.05$) compared to their STZ counterparts. These results demonstrated that STZ-induced T1DM reverses OVX-associated high bone turnover osteoporosis to the type of low bone turnover, leading to greater bone loss and structural defect.

Key words: Type 1 diabetes mellitus, Ovariectomy, Bone turnover, Osteoporosis

Offprint requests to: Minqi Li, Department of Bone Metabolism, School of Stomatology, Shandong University, Shandong Provincial Key Laboratory of Oral Tissue Regeneration, Wenhua West Road 44-1, Jinan 25012, China. e-mail: liminqi@sdu.edu.cn

DOI: 10.14670/HH-18-024

Introduction

With increasing age, multiple metabolic disorders including hypertension, hyperglycemia and hyperlipidemia are likely to occur. Among these disorders, diabetes mellitus (DM) is generally considered to be tightly associated with bone loss and deterioration of bone quality, therefore being regarded as a potential risk factor for osteoporosis (Basaria, 2000; Inaba, 2004).

Insulin-dependent diabetes mellitus, also referred to as type 1 diabetes mellitus (T1DM) (2. Classification and diagnosis of diabetes: Standards of medical care in diabetes-2018, 2018), has been reported to be associated with reduced bone mineral density (BMD), increased risk for osteoporosis and fractures (Tuominen et al., 1999; Janghorbani et al., 2007). Apart from hyperglycemia and its metabolites such as advanced glycation end products, T1DM-associated complications of peripheral neuropathy (Forst et al., 1995), retinopathy (Kayath et al., 1994), and nephropathy (Munoz-Torres et al., 1996) also contribute to osteoporosis. Additionally, Genetic mutations in the vitamin D receptor (Hauache et al., 1998) or collagen type 1α-1 (Hampson et al., 1998)

in T1DM are possibly associated with low BMD.

The deficiency in estrogen after the menopause causes 3% to 5% loss in bone mass every year and ultimately leads to brittle bones and osteoporosis, which is the leading risk factor for bone fracture in aged women (Hui et al., 1990; Black and Rosen, 2016). Several lines of evidence arising from clinical studies suggest that postmenopausal women with T1DM have lower BMD compared with nondiabetic subjects (Rachon et al., 2003; Strotmeyer et al., 2006). Thus, when the patients with postmenopausal-osteoporosis also complicated with T1DM, the pathogenesis of bone metabolism disorder will be more complex. In this case, postmenopausal osteopenia is often aggravated by T1DM, producing more profound impairment on bone quantity and quality.

Based on the differences in bone turnover rate, osteoporosis can be subdivided into high bone turnover osteoporosis and low bone turnover osteoporosis, represented by postmenopausal osteoporosis and senile osteoporosis, respectively. Estrogen deficiency in postmenopausal women leads to increased osteoblastic and osteoclastic ability with the latter far exceeding the former, therefore causing excessive bone resorption and subsequent net bone loss (Garnero et al., 1996, 2000). However, T1DM and its associated complications are shown to inhibit osteoblast differentiation by mesenchymal cells and bone formation activity (Lu et al., 2003; Stolzing et al., 2010), although their actions on osteoclast remain controversial with a suppressive effect being predominant (Gallacher et al., 1993; Hou et al., 1993; Dienelt and zur Nieden, 2011). Therefore, it appears that T1DM-associated osteoporosis is a type of low bone turnover. However, when both pathological conditions, T1DM and estrogen deficiency, coexist in postmenopausal women, which phenotype of bone turnover would be in the ascendant remains unknown. Moreover, although cohort studies support the notion that being concomitant with T1DM significantly exacerbates bone loss and increases risk of suffering from fracture in patients with postmenopausal osteoporosis (Christensen and Svendsen, 1999), the relative mechanisms of T1DM affecting bone remodeling in the context of menopause are still scarcely available. Thus, the aim of this study was to establish a rat model of combination of postmenopausal-osteoporosis with T1DM and to investigate the effect of T1DM on bone structure and bone turnover in estrogen-deficiency rats.

Materials and methods

Animals and treatments

After acclimation for one week, forty 8-week-old female Wistar rats were assigned into four groups (ten rats per group): (i) sham-operated control (SC); (ii) ovariectomized group (OVX); (iii) STZ treated group (STZ); (iv) ovariectomized + STZ treated group (OVX+STZ). The experiments conducted were approved by the Ethical Committee for Animal Research of Shandong University ((1) IAEC No.03/011/04).

After a 7 days' acclimatization period, the rats (OVX and OVX+STZ group) were anesthetized via an intraperitoneal injection of 8% chloral hydrate (400 mg/100 g) and underwent bilateral ovariectomy as reported by Li M et al. (1997). The rats in SC and STZ group received a sham surgery simultaneously as control. Four weeks after the surgery, experimental diabetes was induced as described by Gopalakrishnan et al. (2006). Briefly, the rats were administered a single i.p. dose (50 mg/kg body mass) of STZ (Sigma, St. Louis, Missouri), dissolved in 0.5 mL citrate buffer (0.1 mol/L; pH.4.5). Only animals with consistent blood glucose levels above 13.9 mmol/L were considered diabetic. The fasting blood glucose values and body weight were monitored at 2, 4 and 8 weeks after diabetes induction. At the end of the experiment, all rats were sacrificed. The right tibiae were dissected for micro-CT analysis and the left tibiae were processed for histological, immunohistochemical examination and quantitative real-time PCR.

Micro-CT assessment

12 weeks post-surgery and 8 weeks after STZ injection, the rats from each group were euthanized and subjected to transcardial perfusion with 4% paraformaldehyde in 0.1M phosphate buffer (pH 7.4). The tibiae were carefully dissected free of muscle and connective tissue and subsequently fixed in a solution of 4% buffered paraformaldehyde saline for 24 h in 4°C. The micro-CT system (Inveon Micro-CT, SIEMENS, Germany) was operated at a voltage of 80 KV, and a current of 500 μA was used with a nominal resolution of 10 μm/pixel. The 3D reconstruction images of tibiae were obtained, and the trabecular bone regions of 1mm thickness far from the tibia growth plate were selected as region of interest (ROI) which separated cortical bone from trabecular bone by 3D space filtration of the bone marrow cavity. The structural parameters of ROI such as bone volume fraction (BV/TV, %), trabecular thickness (Tb.Th, μm), trabecular number (Tb.N, 1/mm), trabecular separation (Tb.Sp, μm), trabecular bone pattern factor (Tb.Pf, 1/mm) and bone mineral density (BMD, mg/cm^3), were calculated using Inveon Research Workplace software (SIEMENS, Germany).

Histological study

To process tibiae for histology, paraformaldehyde fixed samples were decalcified by immersion in 10% EDTA (pH 7.4) under constant agitation on a roller mixer at 4°C temperature. The decalcification solution was changed three times a week for 28 days and the samples were subsequently dehydrated in ascending grades of ethanol, cleared in xylene and embedded in paraffin. Sections of 5 μm were cut and stained with

hematoxylin & eosin (H&E), and visualized under a microscope (BX-53, Olympus, Tokyo, Japan).

Immunohistochemical examination and image analysis

Five micrometer-thick paraffin sections were dewaxed in xylene and rehydrated in an ethanol series. Endogenous peroxidases were blocked by incubation in 0.3% hydrogen peroxide for 30 min at room temperature. Then, the sections were pre-incubated with 1% bovine serum albumin (BSA; seologicals proteins Inc. Kankakee, IL, USA) in phosphate-buffered saline for 20 min to reduce non-specific staining. The sections were then incubated for 2 h at room temperature with rabbit anti-tissue-nonspecific alkaline phosphatase (ALP), a gift from professor Oda (Oda et al., 1999), or rabbit anti-cathepsin K antibody (Abcam, Ltd. Hong Kong). After rinsing with PBS, the sections were incubated with horseradish peroxidase-conjugated swine anti-rabbit (DaKo, Glostrup, Denmark) at a dilution of 1:100 for 1 h at room temperature. Immunoreactions were visualized with diaminobenzidine (Sigma-Aldrich, St. Louis, MO, USA). The primary antibody was replaced with PBS for the negative control.

For tartrate-resistant acidic phosphatase (TRAP) staining, the sections were dewaxed in xylene and rehydrated in an ethanol series, then rinsed with PBS and immersed in a solution of 3 mg naphthol AS-BI phosphate, 18 mg red violet LB salt, and 100 mM L (+) tartaric acid (0.36 g) in 30 mL of 0.1 M sodium acetate buffer (pH 5.0) for 15 min at 37°C. Staining was observed by light microscopy after faintly counterstaining with methyl green.

For statistical analysis, 9 tissue sections were selected from each sample and the parameters were expressed as means of parallel samples. Osteoclast numbers were counted, and the mean optical density of ALP, CK, MMP9 staining were measured in three randomly selected non-overlapping microscopic fields in each section by Image-Pro Plus 6.2 software (Media Cybernetics, Silver Spring, MD, USA).

Quantitative real-time PCR

The tibiae were freshly harvested and frozen for storage to prevent degradation. Liquid nitrogen was used to flash freeze the samples and the tibia samples were then pulverized in the Biopulverizer. Total RNA was extracted from samples with RNA iso Plus (Takara Bio Inc, Shiga, Japan). The RNA was eluted with the addition of RNase-free water and an absorbance reading was taken using the nanodrop spectrophotometer to assay RNA concentration. Then RNA samples were reverse transcribed into cDNA with the Prime-Script™ RT reagent Kit (Takara Bio Inc) according to the manufacturer's protocol. Following cDNA synthesis, PCR was performed using primers designed for genes of interest (Table 1). All quantitative reverse transcription-PCRs were performed using Roche LightCycler 480 Real-Time PCR system (Roche, Sussex, UK), and all samples were run in triplicate. The cycling conditions were as follows: 40 cycles of 95°C for 3 s and 60°C for 30 s. Relative quantities of the tested genes were normalized to GAPDH mRNA. Analysis of the relative quantitation required calculations based on the threshold cycle, i.e. the cycle number at which the amplification plot crosses a fixed threshold above the baseline (Ct). Relative quantitation was performed using the comparative $\Delta\Delta$Ct method according to the manufacturer's instructions.

Statistical analysis

After testing the results for normality using the Kolmogrov-Smirnov test, one-way analysis of variance (ANOVA) followed by the Least Significant Difference (LSD) post-test was applied to the data sets of structural parameters, osteoclast numbers and immunostaining density. For each group, the correlations of time with fasting blood glucose values or body weight were tested using a multi-factor analysis of variance for repeated measures. Statistical analysis was performed using SPSS 12.0 software (SPSS Inc., Chicago, Illinois, USA). Results were expressed as mean ± standard deviation. Differences were considered statistically significant at $P<0.05$.

Results

Fasting blood glucose and body weight monitoring

We recorded the level of fasting blood glucose and body weight of rats in each group during the experiment (Fig. 1A-D). As expected, the blood glucose values of rats with STZ injection reached beyond 14 mmol/L and maintained for up to 8 weeks, along with a gradually

Table 1. Oligonucleotide primers used for quantitative real-time PCR.

Gene name		Oligonucleotide Sequence (5'→3')
RANKL	Forward	GAAACCTCAGGGAGCGTACC
	Reverse	AACAGGGAAGGGTTGGACAC
OPG	Forward	TGCTCCTGGCACCTACCTAA
	Reverse	TCACATTCGCACACTCGGTT
TRAF6	Forward	AGAGGAATCACTTGGCACGG
	Reverse	TCTGCGTTTCCATTTTGGCG
NF-κB	Forward	CCCACGGATGTTCACAGACA
	Reverse	CTGTCGGAGAAGTTGGGCAT
LRP5	Forward	AGATGTGGATCAGCAAGCAG
	Reverse	GCGCAAGTTAGGTTTTGTCA
β-catenin	Forward	CCATTGTGTTGCACCCTGTG
	Reverse	CCGCTTTGTCCCGTCTATGT
Runx2	Forward	CCTCAGTGATTTAGGGCGCA
	Reverse	GGTGGAATGGATGGATGGGG
β-actin	Forward	AGATGTGGATCAGCAAGCAG
	Reverse	GCGCAAGTTAGGTTTTGTCA

decreased body weight, indicating the successful establishment of STZ rats model. OVX rats had normal level of blood glucose and exhibited a greater body weight gain over time with respect to SC rats.

Bone histomorphometric analysis by Micro-CT

Next, the effect of OVX and STZ alone or in combination on bone phenotype was evaluated by means of Micro-CT. The longitudinal sections and 3D reconstruction images of trabecular bone at the proximal tibia were shown in Fig. 2A-H. OVX rats showed particularly sparse and poorer connected trabeculae, along with compensatory thickened trabecular bone compared with SC rats. Although the bone mass seemed to be unchanged in STZ rats, the trabeculae thickness appeared to be slightly decreased in comparison with SC group. When OVX and STZ were combinedly used, the microarchitecture of tibia was most seriously deteriorated as evidenced by the total absence of trabeculae at the core region and extremely sparse distribution of trabeculae at the peripheral area of metaphysis.

Bone structural parameters were analyzed based on the data from Micro-CT. For BMD and Tb.Th, SC rats exhibited highest values, followed by OVX and STZ rats and leaving OVX+STZ rats at the lowest level (Fig. 2I,K). BV/TV among groups showed the same trend with Tb.N as depicted in Fig. 2J,L, where STZ caused a slight decrease in both parameters compared with SC rats, followed by OVX rats and the combination group revealed the greatest reduction in BV/TV and Tb.N. Tb.Sp was negatively correlated with BV/TV and Tb.N among groups, where higher Tb.Sp corresponded to lower BV/TV and Tb.N, as shown in Fig. 2M. Tb.Pf is a new histomorphometric parameter reflecting the relation of convex to concave surfaces of trabeculae. A lower Tb.Pf represents a well-connected spongy lattice, whereas a higher Tb.Pf indicates a badly connected trabecular lattice. As shown in Fig. 2N, Tb.Pf was higher in rats with either OVX or STZ treatment than in SC rats, with its highest value detected in OVX+STZ group.

Histological examination, Immunohistochemistry for ALP and gene expression of Wnt/β-catenin signaling pathway

As shown in Fig. 3A,B, compared with the SC rats, OVX rats showed decreased trabecula number and increased trabecula separation in tibia metaphysis, along with thickened trabecular bone in appearance. The

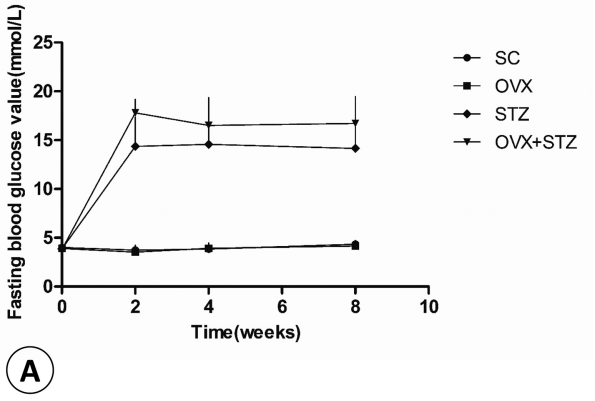

A

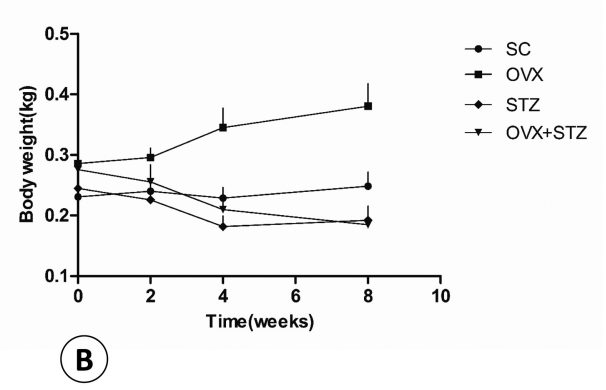

B

Group	R	P
SC	0.241	0.139
OVX	0.219	0.152
STZ	0.579	0.001
OVX+STZ	0.536	0.002

C

Group	R	P
SC	0.213	0.185
OVX	0.819	＜0.001
STZ	-0.712	0.001
OVX+STZ	-0.829	＜0.001

D

Fig. 1. Monitoring the levels of fasting blood glucose and body weight. The fasting blood glucose **(A)** and body weight **(B)** of rats in each group was recorded every two weeks. The correlation between fasting blood glucose and time **(C)** as well as body weight and time **(D)** were also analyzed.

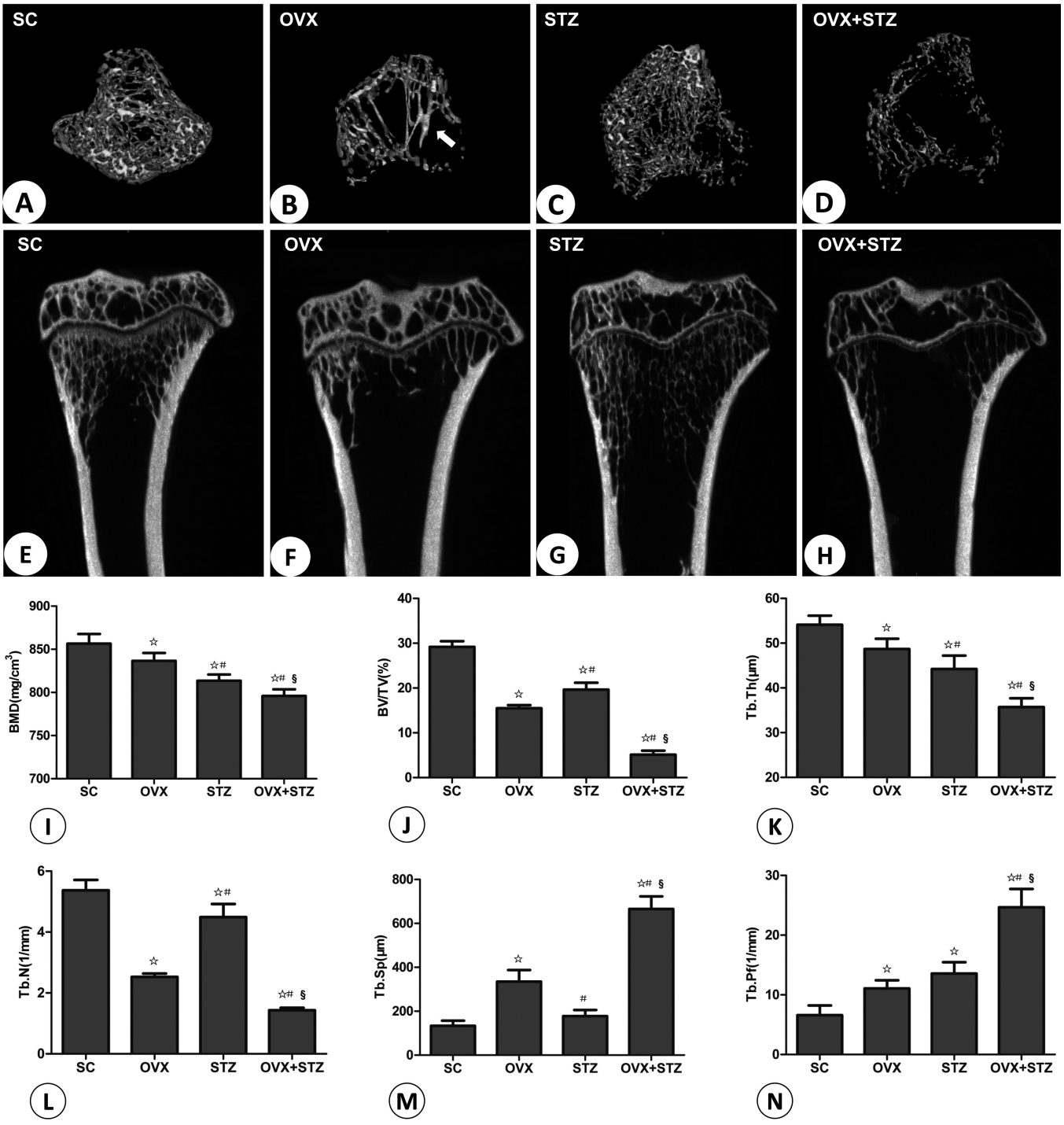

Fig. 2. Representative Micro-CT images of trabecular bone microarchitecture in the proximal tibia and histomorphometric analysis. The 3D reconstruction images **(A-D)** and longitudinal sections (**E-H)** of proximal tibiae for each group. The histomorphometric parameters of ROI region such as bone mineral density (BMD), bone volume fraction (BV/TV), trabecular thickness (Tb.Th), trabecular number (Tb.N), trabecular separation (Tb.Sp) and trabecular bone pattern factor (Tb.Pf) were analyzed **(I-N)**. ☆, compared with the SC group; #, compared with the OVX group; §, compared with the STZ group (P<0.05).

number and morphologic features of tibia trabecula of STZ rats were similar to those of OVX rats except a notably decreased trabecula thickness and thinner growth plate (Fig. 3C). When OVX and STZ were combined, the rats displayed most serious bone loss characterized by extremely reduced trabecula number and island-like trabecular morphology (Fig. 3D). These results suggest that OVX+STZ rats suffer more from bone loss compared with solely diseased subjects.

Immunohistochemistry staining for ALP was used to assess osteoblastic activity. As shown in Fig. 3E and F, ALP staining was stronger in OVX rats relative to SC rats, especially at the surface of trabecula bone where the osteoblasts located. However, STZ rats exhibited highly suppressed ALP immunoreactivity compared with SC and OVX groups (Fig. 3G). The weakest immunostaining of ALP was found for tibia of OVX+STZ rats where few ALP positive osteoblasts were only found at the lower edge of the growth plate and ALP immunolabeling was hardly seen at the surface of trabecula (Fig. 3H). The immunostaining intensity of ALP in each group is statistically summarized in Fig. 3I.

To confirm whether Wnt/β-catenin pathway, which is crucial for osteoblastic differentiation, would be affected by OVX and/or STZ treatment, RT-qPCR for LRP5 and β-catenin were performed. As shown in Fig. 3J and K, gene expressions of LRP5 and β-catenin were strongly enhanced in OVX rats, whereas STZ treated rats showed slightly attenuated mRNA expression of LRP5 and β-catenin in comparison with the control. OVX rats concomitantly treated with STZ exhibited further compromised activation of Wnt/β-catenin pathway. Consistently, as one of the most important osteoblastic transcriptional factors, Runx2 gene expression was also potentiated by OVX and reduced by

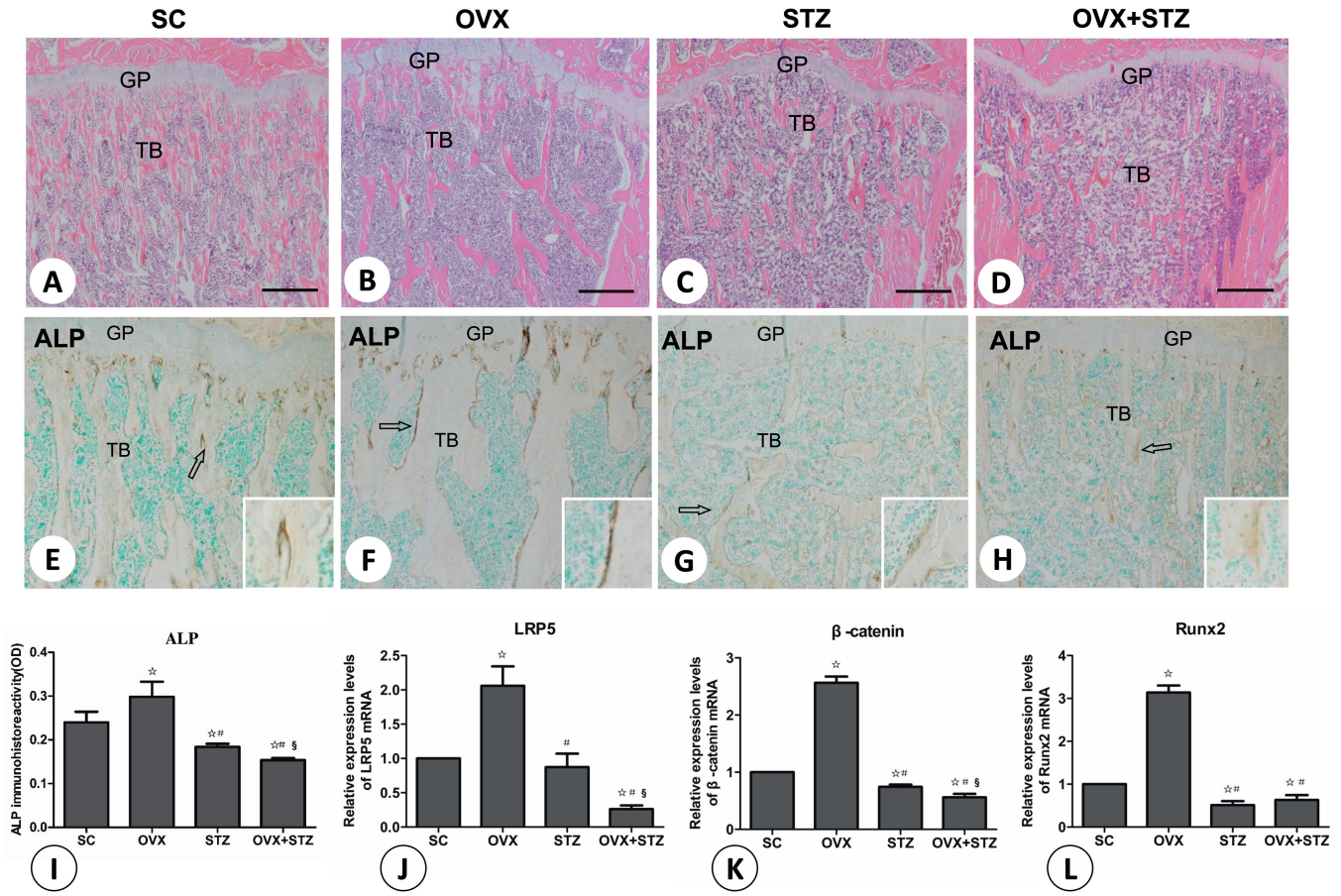

Fig. 3. Histological alterations and Immunohistochemistry staining for alkaline phosphatase (ALP) and statistical analysis. Representative HE staining images of mesial tibiae for SC **(A),** OVX (**B**), STZ (**C**) and OVX+STZ **(D)** group. Representative ALP immunostaining images in SC **(E)**, OVX **(F)**, STZ **(G)** and OVX+STZ **(H)** group are presented on the lower panel. For E-H, the figure in the lower right corner is the higher magnification of the area indicated by the open arrow. **I** is the statistical graph for ALP immunoactivity of each group. Total RNA was extracted from the tibiae and subjected to quantitative real time PCRs using probes specific for LRP-5 **(J)**, β-catenin **(K)** and Runx2 **(L)**. GAPDH served as the control. TB trabecula bone. GP growth plate. Bar 50μm. ☆, compared with the SC group; #, compared with the OVX group; §, compared with the STZ group ($P<0.05$).

treatment with STZ alone or cotreatment with OVX and STZ (Fig. 3L). Together, the above results suggested that osteoblastic activity is enhanced by OVX and suppressed by STZ treatment. Importantly, STZ-induced suppressive effect on osteoblastic activity evidently exceeds the promotive effect resulting from OVX when both conditions coexist.

TRAP staining and Immunohistochemistry for CK

As shown in Fig. 4A,B, compared with SC group, OVX rats had a significantly increased number of TRAP-positive osteoclasts which were larger in size and principally observed below the growth plate. On the contrary, the rats with STZ exhibited diminished number

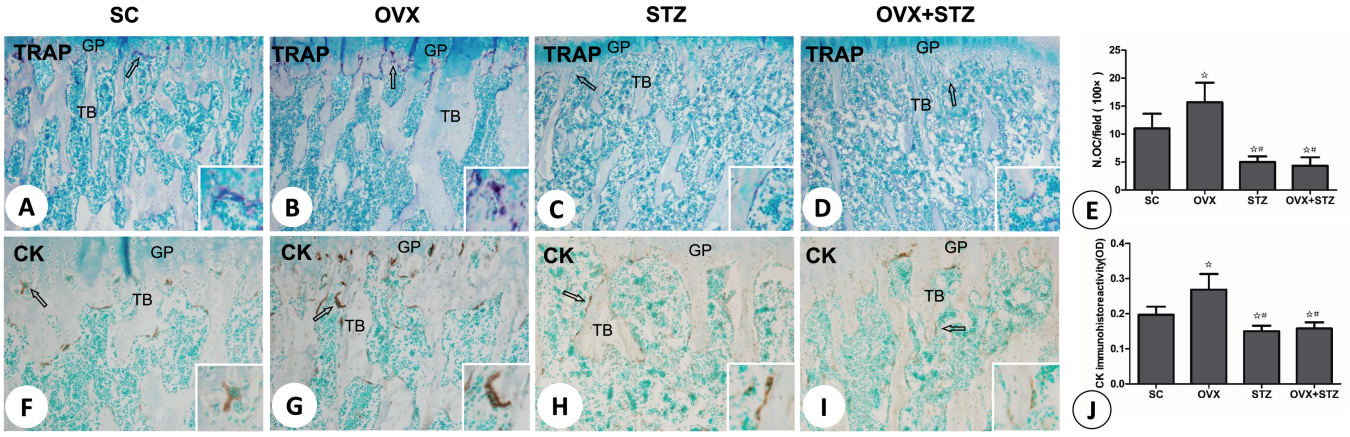

Fig. 4. TRAP staining and Immunohistochemistry for CK and statistical analysis. The distribution of TRAP-positive osteoclasts located at the border of trabecular bone in SC **(A)**, OVX **(B)**, STZ **(C)** and OVX+STZ **(D)** group. Representative CK immunostaining images for osteoclasts in SC **(F)**, OVX **(G)**, STZ **(H)** and OVX+STZ **(I)** group are presented on the lower panel. For A-D and F-I, the figure in the lower right corner is the higher magnification of the area indicated by the open arrow. **E** and **J** are the statistical graphs for the number of TARP-positive osteoclasts and immunoactivity of CK in each group. TB trabecula bone. GP growth plate. ☆, compared with the SC group; #, compared with the OVX group (P<0.05).

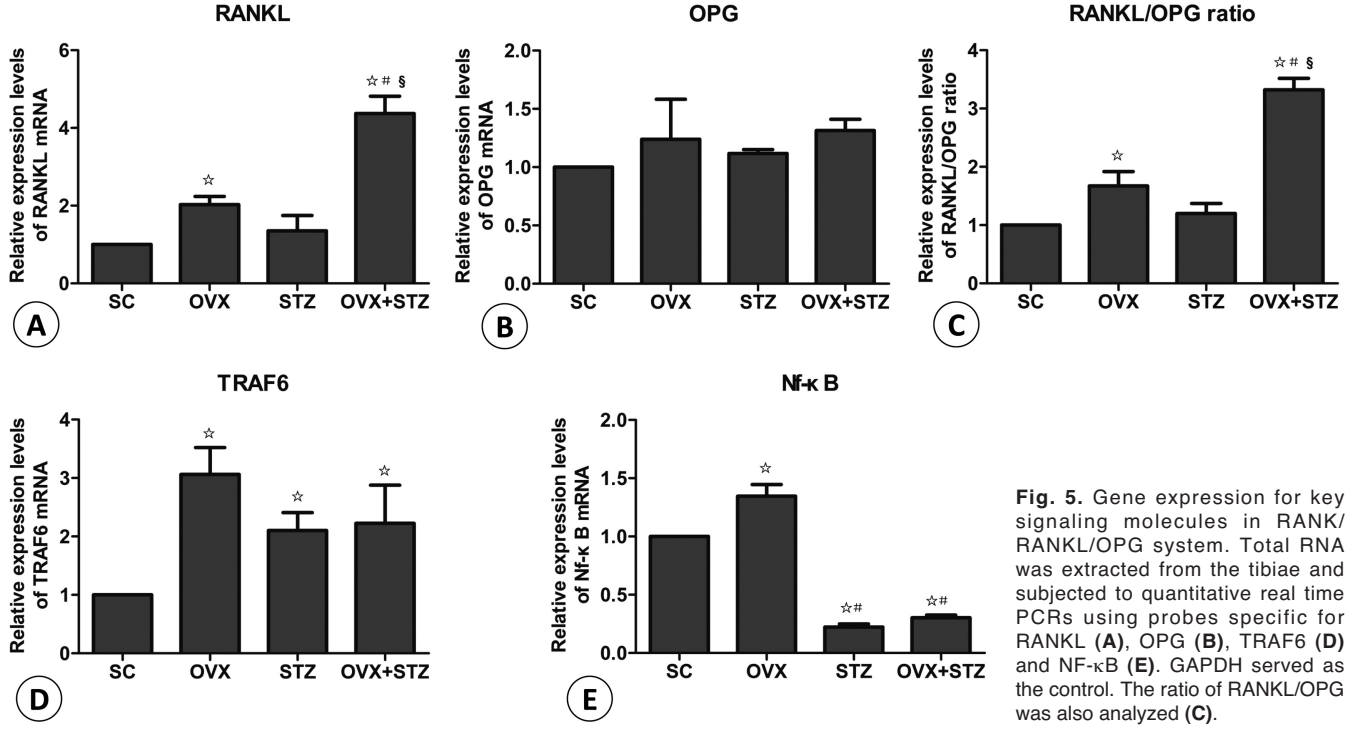

Fig. 5. Gene expression for key signaling molecules in RANK/RANKL/OPG system. Total RNA was extracted from the tibiae and subjected to quantitative real time PCRs using probes specific for RANKL **(A)**, OPG **(B)**, TRAF6 **(D)** and NF-κB **(E)**. GAPDH served as the control. The ratio of RANKL/OPG was also analyzed **(C)**.

of TRAP-positive osteoclasts in comparison with SC group (Fig. 4C). Being concomitant with OVX did not make a difference in osteoclast number in relative to rats with STZ alone (Fig. 4D). Consistent with the results of TRAP staining, immunolabeling of CK was remarkably stronger in OVX group than in SC group (Fig. 4E,F). In contrast, CK expression was strongly suppressed in rats with STZ, with no significant differences between STZ group and OVX+STZ group (Fig. 4G,H). The statistical results for the number of TRAP-positive osteoclasts and OD value of CK immunolabeling are presented in Fig. 4E,J, respectively.

Gene expression of key molecules in RANKL-RANK signaling pathway

Considering the vital role of RANKL-RANK signaling pathway in activation of osteoclastic differentiation, the gene expression levels of several key molecules in this signaling pathway were tested by RT-qPCR using fresh samples. The results showed that the expression of RANKL mRNA doubled in OVX rats and was robustly increased by 3-fold in OVX+STZ rats. STZ alone slightly enhanced RANKL mRNA expression without statistical significance (Fig. 5A). However, the decoy receptor for RANKL-OPG appeared unaffected by OVX and/or STZ treatment (Fig. 5B). RANKL/OPG ratio exhibited a similar changing pattern as RANKL did (Fig. 5C). The gene expression of TRAF6, the signal transducer downstream of RANK, was remarkably upregulated by OVX and/or STZ treatment to a similar extent (Fig. 5D). NF-κB mRNA expression was remarkably enhanced by OVX but less potentiated by STZ injection or concomitant treatment (Fig. 5E).

Discussion

In the present study, we histologically assessed the effect of estrogen deficiency and T1DM alone or in combination on the osteoblast and osteoclast-mediated bone remodeling in rats and observed that OVX-induced estrogen deficiency caused osteoporosis with an increased bone turnover whereas T1DM resulted in bone loss with a decreased bone turnover. When both pathological conditions were combined, the bone loss and deterioration would be further aggravated and STZ-associated low level of bone turnover would entirely prevail over the effect of estrogen deficiency.

The rats which received ovariectomy in our study exhibited a slight increase in body weight and significant bone loss featured by compromised bone histomorphometric parameters including lower BMD, wider trabeculae separation and reduced trabeculae thickness and number in long bone which are in line with previous studies (Yamazaki and Yamaguchi, 1989; Comelekoglu et al., 2007). Although the bone mass and trabeculae number weren't obviously changed in STZ rats, the trabeculae thickness appeared to be slightly decreased and broken in comparison with SC and OVX rats, revealing impaired bone formation capacity of osteoblast due to insulin deficiency, which is basically consistent with the data from other animal models studies (Follak et al., 2004; Erdal et al., 2012). Specifically, coexistence of OVX and STZ-induced T1DM appeared to synergistically reduce bone mass and deteriorate bone structural properties in comorbid animals, since various indices of bone histomorphometry in OVX+STZ rats showed the minimum values among groups. A previous study in rats with OVX and/or STZ-induced diabetes

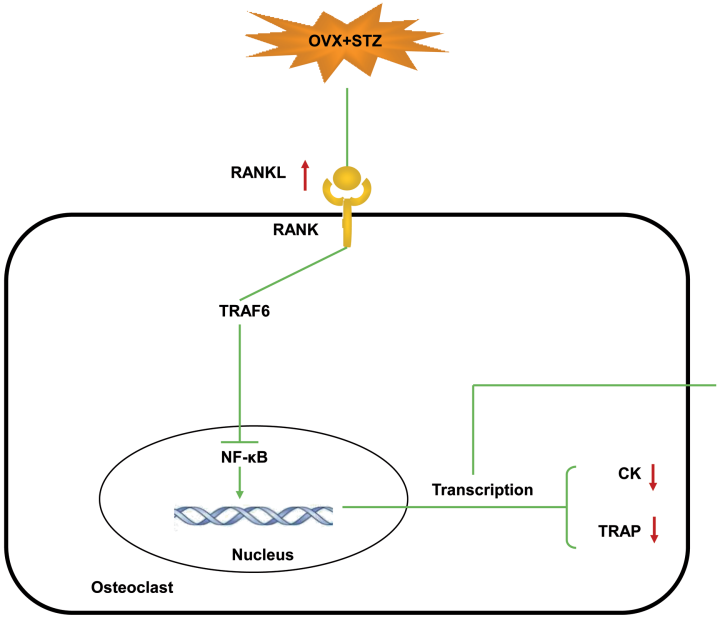

Fig. 6. Schematic model of the combined action of OVX and STZ on RANKL-RANK signaling pathway and osteoclastogenesis. OVX-induced estrogen deficiency increases RANKL production and the following NF-κB activation and nuclear translocation, therefore highly promoting osteoclast differentiation and activation, which manifests as osteoporosis with high bone turnover. When T1DM concomitantly occurs, RANKL-RANK signaling pathway, especially NF-κB activation is inhibited although RANKL production is further enhanced. Subsequently, production of osteoclastic enzymes including TRAP and CK as well as osteoclast differentiation are downregulated and osteoporosis with low bone turnover occurs.

demonstrated a significantly greater decrease in bone volume in combined group than in single-loaded group at 6-month post-surgery, which is consistent with our results (Nagasawa, 1995). Despite this, there have been studies pointing out that although being markedly detected, bone loss in ovariectomized diabetic rats was not more marked or even less than that caused by diabetes or ovariectomy alone (Verhaeghe et al., 1994; Herrero et al., 1998). This discrepancy could be partially explained by the differences in species of rats used and the selection of lumbar vertebrae or tibiae for histomorphological analysis.

Impaired osteoblast differentiation and activity are commonly observed and crucial for the compromised bone structural and mechanical properties in patients with some types of osteoporosis. However, in other types of osteoporosis such as postmenopausal osteoporosis, osteoblastic differentiation and activity are both enhanced with more potentiated osteoclastic formation and activity, leading to bone loss in general, just as exhibited by the OVX rats in the present study. Using immunohistochemistry approach, increased expression of ALP, the most critical functional enzyme produced by osteoblast, was identified in OVX rats, confirming the strengthened osteoblast, a typical feature of high bone turnover osteoporosis. However, for T1DM associated bone deterioration, there has been evidence showing that it is the defect of osteoblast differentiation and function rather than osteoclastic over-function that should be responsible for osteoporosis. Clinical studies consistently demonstrated a decrease of type 1 collagen (PICP) in subjects with T1DM (Gunczler et al., 1998, 2001). Animal model studies using the streptozotocin induced T1DM rats showed that the mesenchymal stem cells possess impaired potential for self-renewal as well as osteoblastic differentiation, possibly due to insulin deficiency and hyperglycemia (Lu et al., 2003; Dienelt and zur Nieden, 2011; Fulzele and Clemens, 2012). Consistent with these findings, our results revealed significantly reduced expression of ALP on the surface of the trabecula in STZ rats as compared to SC group, highlighting the suppressed osteoblast differentiation and defective osteoblast activity in these animals. However, clinical and in vivo studies on ALP activity alterations following T1DM are controversial, with higher (Olmos et al., 1994; Miazgowski and Czekalski, 1998), similar (Gerdhem et al., 2005) and lower (Kemink et al., 2000) in related to healthy subjects being recorded. This inconsistency may be due to the differences in gender, age, race or medication treatment of the patients recruited. Specifically, insulin is an anabolic agent in bone formation. In animal study, STZ-induced destruction of the insulin-producing β-cells in the pancreas leads to insulin deficiency and subsequent impaired bone formation. For human T1DM patients, insulin injection is routinely used to control blood glucose and the bone formation ability would be partly rescued. But regarding experimental animals, they do not take insulin and mimic poorly controlled T1MD in human, which may be an important cause for the significant reduced ALP activity in bone tissue. Interestingly, it is unexpected that OVX+STZ rats exhibited the minimum value in ALP immunostaining intensity among all groups rather than some intermediate value between OVX and STZ group. By analyzing serum level of bone gamma-carboxyglutamic-acid-containing proteins (BGP), a bone formation marker, Herrero et al noted a similar bone formation rate in ovariectomized diabetic rats to that in rats with diabetes alone (Herrero et al., 1998). The causes which contribute to these conflicting findings to osteoblast activity and bone formation remains unclear.

Estrogen deficiency leads to highly potentiated osteoclast differentiation and activity accompanied by less enhanced osteoblast activation, which is recognized as the major contributor to postmenopausal osteoporosis (Khosla, 2010). Consistently, immunostaining for osteoclastic marker enzymes including TRAP and CK substantiated the increased number and lifted activity of osteoclasts in OVX rats. The contrary happened to rats with T1DM where the expression of osteoclastic marker enzymes was remarkably decreased compared to SC group, indicating the suppressive effect of T1DM on osteoclast. Unlike the effects of T1DM on osteoblasts, the data on the role of T1DM in osteoclast function remains contradictory. Dienelt et al reported decreased osteoclastic differentiation potential by embryonic stem cells in hyperglycemic versus physiological culture medium (Dienelt and zur Nieden, 2011). Animal studies also revealed a reduced number of osteoclasts at the femoral neck region of untreated T1DM rats compared to nondiabetic controls (Hou et al., 1993). In contrast, bone marrow-derived osteoclasts isolated from T1DM rats exhibited increased bone resorption activity under stimulation of receptor activator of nuclear factor kappa-B ligand (RANKL). Consistently, increased bone resorption was found in rat model of T1DM likely due to a reduction in osteoprotegerin (OPG) expression, a decoy receptor for RANKL (Silva et al., 2012). In this study, STZ-induced T1DM resulted in significantly suppressed osteoclastic activity in rats and whether these unconformities were due to differences in animal species, age, gender, or markers used was unclear. Specifically, it appeared that the inhibitory action of T1DM on osteoclast was not affected by the presence of OVX-associated estrogen deficiency as no differences in osteoclast specific enzymes was noted between STZ and concomitant groups.

Estrogen has been shown to inhibit osteoclastogenesis through suppressing RANK signaling pathway (Robinson et al., 2009). Consistently, our data revealed an increase in the gene expression of RANKL, TRAF6 and NF-κB in OVX rats. In keeping with the immunostaining of osteoclastic enzyme, STZ induced T1DM rats showed inhibited RANK signaling activation as evidenced by the decreased NF-κB gene expression, although RANKL and RANKL/OPG ratio was unchanged. Interestingly, when OVX and STZ

combined, the rats exhibited highly elevated RANKL and RANKL/OPG ratio, however, NF-κB gene expression was reduced to an extremely low level which indicates the RANK signaling pathway was strongly suppressed. These findings suggest that both OVX and STZ treatment lead to RANKL/OPG ratio increasing but their effect on RANK signaling pathway is contrary. OVX-associated estrogen deficiency induces the activation of RANK signaling pathway while STZ-induced T1DM inhibits it, but the inhibitory effect overwhelmingly outstrips the supportive effect when both conditions are combined.

Since T1DM is caused by a deficiency of insulin, insulin replacement is the mainstay of treatment for patients with T1DM. However, increased risk of hypoglycemia and insulin resistance are increasingly recognized as obstacles to glycemic control in T1DM. Thus, some antidiabetic agents approved for T1DM have been tried to improve clinical outcomes and reduce total daily dose of insulin (Bhat et al., 2007). Based on the results of the present study that OVX+STZ rats showed serious bone destruction even worse than their sole OVX counterparts, some medications such as glitazone and diuretics should be avoided in postmenopausal women with T1DM as these medications are reported to be linked to low bone mass thus may potentially increase the risk of fracture (Rejnmark et al., 2006; Bazelier et al., 2013).

In conclusion, we demonstrated that T1DM associated osteoporosis was a type of low bone turnover featured by decreased activity of both osteoblast and osteoclast, which is contrary to that of postmenopausal osteoporosis. When both pathologies coexisted, T1DM induced low bone turnover would overwhelmingly prevail over estrogen deficiency-associated high bone turnover and ultimately caused more aggravated osteoporosis, which means postmenopausal women with T1DM are at higher risk of fracture. Thus, earlier and more active bone screening is needed among this population with the goal of preventing fracture and subsequent morbidity and mortality.

Acknowledgements. This study was partially supported by the National Nature Science Foundation of China (grant No. 81470719; 81611140133) to Minqi Li, and the Shandong Province Medicine and Health Science Technology Development Foundation, China (grant No. 2017WS649) and the Doctoral Research Start-up Fund of Jining Medical University, China (grant No. 2017JYQD26) to Bo Liu.

Declaration of interest. All authors declare that they have no conflict of interest.

References

Basaria S. (2000). Link between diabetes and osteoporosis. Diabetes Care 23, 564-565.

Bazelier M.T., de Vries F., Vestergaard P., Herings R.M., Gallagher A.M., Leufkens H.G. and van Staa T.P. (2013). Risk of fracture with thiazolidinediones: An individual patient data meta-analysis. Front. Endocrinol. 4, 11.

Bhat R., Bhansali A., Bhadada S. and Sialy R. (2007). Effect of pioglitazone therapy in lean type 1 diabetes mellitus. Diabetes Res. Clin. Pract. 78, 349-354.

Black D.M. and Rosen C.J. (2016). Clinical practice. Postmenopausal osteoporosis. N. Engl. J. Med. 374, 254-262.

Christensen J.O. and Svendsen O.L. (1999). Bone mineral in pre- and postmenopausal women with insulin-dependent and non-insulin-dependent diabetes mellitus. Osteoporos. Int. 10, 307-311.

Classification and diagnosis of diabetes: Standards of medical care in diabetes-2018. (2018). Diabetes Care 41, S13-s27.

Comelekoglu U., Bagis S., Yalin S., Ogenler O., Yildiz A., Sahin N.O., Oguz I. and Hatungil R. (2007). Biomechanical evaluation in osteoporosis: Ovariectomized rat model. Clin. Rheumatol. 26, 380-384.

Dienelt A. and zur Nieden N.I. (2011). Hyperglycemia impairs skeletogenesis from embryonic stem cells by affecting osteoblast and osteoclast differentiation. Stem Cells Dev. 20, 465-474.

Erdal N., Gurgul S., Demirel C. and Yildiz A. (2012). The effect of insulin therapy on biomechanical deterioration of bone in streptozotocin (STZ)-induced type 1 diabetes mellitus in rats. Diabetes Res. Clin. Pract. 97, 461-467.

Follak N., Kloting I., Wolf E. and Merk H. (2004). Improving metabolic control reverses the histomorphometric and biomechanical abnormalities of an experimentally induced bone defect in spontaneously diabetic rats. Calcif. Tissue Int. 74, 551-560.

Forst T., Pfutzner A., Kann P., Schehler B., Lobmann R., Schafer H., Andreas J., Bockisch A. and Beyer J. (1995). Peripheral osteopenia in adult patients with insulin-dependent diabetes mellitus. Diabet. Med. 12, 874-879.

Fulzele K. and Clemens T.L. (2012). Novel functions for insulin in bone. Bone 50, 452-456.

Gallacher S.J., Fenner J.A., Fisher B.M., Quin J.D., Fraser W.D., Logue F.C., Cowan R.A., Boyle I.T. and MacCuish A.C. (1993). An evaluation of bone density and turnover in premenopausal women with type 1 diabetes mellitus. Diabet. Med. 10, 129-133.

Garnero P., Sornay-Rendu E., Chapuy M.C. and Delmas P.D. (1996). Increased bone turnover in late postmenopausal women is a major determinant of osteoporosis. J. Bone Miner. Res. 11, 337-349.

Garnero P., Sornay-Rendu E., Claustrat B. and Delmas P.D. (2000). Biochemical markers of bone turnover, endogenous hormones and the risk of fractures in postmenopausal women: The ofely study. J. Bone Miner. Res. 15, 1526-1536.

Gerdhem P., Isaksson A., Akesson K. and Obrant K.J. (2005). Increased bone density and decreased bone turnover, but no evident alteration of fracture susceptibility in elderly women with diabetes mellitus. Osteoporos. Int. 16, 1506-1512.

Gopalakrishnan V., Arunakaran J., Aruldhas M.M. and Srinivasan N. (2006). Effects of streptozotocin-induced diabetes mellitus on some bone turnover markers in the vertebrae of ovary-intact and ovariectomized adult rats. Biochem. Cell Biol. 84, 728-736.

Gunczler P., Lanes R., Paz-Martinez V., Martins R., Esaa S., Colmenares V. and Weisinger J.R. (1998). Decreased lumbar spine bone mass and low bone turnover in children and adolescents with insulin dependent diabetes mellitus followed longitudinally. J. Pediatr. Endocrinol. Metab. 11, 413-419.

Gunczler P., Lanes R., Paoli M., Martinis R., Villaroel O. and Weisinger J.R. (2001). Decreased bone mineral density and bone formation markers shortly after diagnosis of clinical type 1 diabetes mellitus. J.

Pediatr. Endocrinol. Metab. 14, 525-528.

Hampson G., Evans C., Petitt R.J., Evans W.D., Woodhead S.J., Peters J.R. and Ralston S.H. (1998). Bone mineral density, collagen type 1 alpha 1 genotypes and bone turnover in premenopausal women with diabetes mellitus. Diabetologia 41, 1314-1320.

Hauache O.M., Lazaretti-Castro M., Andreoni S., Gimeno S.G., Brandao C., Ramalho A.C., Kasamatsu T.S., Kunii I., Hayashi L.F., Dib S.A. and Vieira J.G. (1998). Vitamin D receptor gene polymorphism: Correlation with bone mineral density in a brazilian population with insulin-dependent diabetes mellitus. Osteoporos. Int. 8, 204-210.

Herrero S., Calvo O.M., Garcia-Moreno C., Martin E., San Roman J.I., Martin M., Garcia-Talavera J.R., Calvo J.J. and del Pino-Montes J. (1998). Low bone density with normal bone turnover in ovariectomized and streptozotocin-induced diabetic rats. Calcified Tissue Int. 62, 260-265.

Hou J.C., Zernicke R.F. and Barnard R.J. (1993). Effects of severe diabetes and insulin on the femoral neck of the immature rat. J. Orthop. Res. 11, 263-271.

Hui S.L., Slemenda C.W. and Johnston C.C. Jr (1990). The contribution of bone loss to postmenopausal osteoporosis. Osteoporos. Int. 1, 30-34.

Inaba M. (2004). Secondary osteoporosis: Thyrotoxicosis, rheumatoid arthritis, and diabetes mellitus. J. Bone Miner. Metab. 22, 287-292.

Janghorbani M., Van Dam R.M., Willett W.C. and Hu F.B. (2007). Systematic review of type 1 and type 2 diabetes mellitus and risk of fracture. Am. J. Epidemiol. 166, 495-505.

Kayath M.J., Dib S.A. and Vieira J.G. (1994). Prevalence and magnitude of osteopenia associated with insulin-dependent diabetes mellitus. J. Diabetes Complications 8, 97-104.

Kemink S.A., Hermus A.R., Swinkels L.M., Lutterman J.A. and Smals A.G. (2000). Osteopenia in insulin-dependent diabetes mellitus; prevalence and aspects of pathophysiology. J. Endocrinol. Invest. 23, 295-303.

Khosla S. (2010). Update on estrogens and the skeleton. J. Clin. Endocrinol. Metab. 95, 3569-3577.

Li M., Shen Y. and Wronski T.J. (1997). Time course of femoral neck osteopenia in ovariectomized rats. Bone 20, 55-61.

Lu H., Kraut D., Gerstenfeld L.C. and Graves D.T. (2003). Diabetes interferes with the bone formation by affecting the expression of transcription factors that regulate osteoblast differentiation. Endocrinology 144, 346-352.

Miazgowski T. and Czekalski S. (1998). A 2-year follow-up study on bone mineral density and markers of bone turnover in patients with long-standing insulin-dependent diabetes mellitus. Osteoporos. Int. 8, 399-403.

Munoz-Torres M., Jodar E., Escobar-Jimenez F., Lopez-Ibarra P.J. and Luna J.D. (1996). Bone mineral density measured by dual x-ray absorptiometry in spanish patients with insulin-dependent diabetes mellitus. Calcified Tissue Int. 58, 316-319.

Nagasawa T. (1995). Bone histomorphometric osteopenia induced by ovariectomy or diabetes mellitus in rat. Nihon Seikeigeka Gakkai zasshi 69, 699-707. (In Japanese)

Oda K., Amaya Y., Fukushi-Irie M., Kinameri Y., Ohsuye K., Kubota I., Fujimura S. and Kobayashi J. (1999). A general method for rapid purification of soluble versions of glycosylphosphatidylinositol-anchored proteins expressed in insect cells: An application for human tissue-nonspecific alkaline phosphatase. J. Biochem. 126, 694-699.

Olmos J.M., Perez-Castrillon J.L., Garcia M.T., Garrido J.C., Amado J.A. and Gonzalez-Macias J. (1994). Bone densitometry and biochemical bone remodeling markers in type 1 diabetes mellitus. Bone Miner. 26, 1-8.

Rachon D., Mysliwska J., Suchecka-Rachon K., Semetkowska-Jurkiewicz B., Zorena K. and Lysiak-Szydlowska W. (2003). Serum interleukin-6 levels and bone mineral density at the femoral neck in post-menopausal women with type 1 diabetes. Diabet. Med. 20, 475-480.

Rejnmark L., Vestergaard P., Heickendorff L., Andreasen F. and Mosekilde L. (2006). Loop diuretics increase bone turnover and decrease bmd in osteopenic postmenopausal women: Results from a randomized controlled study with bumetanide. J. Bone Miner. Res. 21, 163-170.

Robinson L.J., Yaroslavskiy B.B., Griswold R.D., Zadorozny E.V., Guo L., Tourkova I.L. and Blair H.C. (2009). Estrogen inhibits rankl-stimulated osteoclastic differentiation of human monocytes through estrogen and rankl-regulated interaction of estrogen receptor-alpha with bcar1 and traf6. Exp. Cell Res. 315, 1287-1301.

Silva J.A., Lopes Ferrucci D., Peroni L.A., de Paula Ishi E., Rossa-Junior C., Carvalho H.F. and Stach-Machado D.R. (2012). Periodontal disease-associated compensatory expression of osteoprotegerin is lost in type 1 diabetes mellitus and correlates with alveolar bone destruction by regulating osteoclastogenesis. Cells, Tissues, Organs 196, 137-150.

Stolzing A., Sellers D., Llewelyn O. and Scutt A. (2010). Diabetes induced changes in rat mesenchymal stem cells. Cells Tissues Organs 191, 453-465.

Strotmeyer E.S., Cauley J.A., Orchard T.J., Steenkiste A.R. and Dorman J.S. (2006). Middle-aged premenopausal women with type 1 diabetes have lower bone mineral density and calcaneal quantitative ultrasound than nondiabetic women. Diabetes Care 29, 306-311.

Tuominen J.T., Impivaara O., Puukka P. and Ronnemaa T. (1999). Bone mineral density in patients with type 1 and type 2 diabetes. Diabetes Care 22, 1196-1200.

Verhaeghe J., Suiker A.M., Einhorn T.A., Geusens P., Visser W.J., Van Herck E., Van Bree R., Magitsky S. and Bouillon R. (1994). Brittle bones in spontaneously diabetic female rats cannot be predicted by bone mineral measurements: Studies in diabetic and ovariectomized rats. J. Bone Miner. Res. 9, 1657-1667.

Yamazaki I. and Yamaguchi H. (1989). Characteristics of an ovariectomized osteopenic rat model. J. Bone Miner. Res. 4, 13-22.

Accepted July 11, 2018